Hindawi
International Transactions on Electrical Energy Systems
Volume 2022, Article ID 9971609, 10 pages
https://doi.org/10.1155/2022/9971609

*Research Article*

# Novel Passive Islanding Detection Technique by Monitoring Reverse Power at PCC

**Muhammad Usman,[1] Safdar Raza,[1] Hafiz Mudassir Munir,[2] Mughees Riaz,[1] Syed Sabir Hussain Bukhari,[2] and Jong-Suk Ro[3,4]**

[1]*Department of Electrical Engineering, NFC Institute of Engineering & Technology, Multan, Punjab, Pakistan*
[2]*Department of Electrical Engineering, Sukkur IBA University, Sukkur 65200, Pakistan*
[3]*Department of Intelligent Energy and Industry, Chung-Ang University, Seoul 06910, Republic of Korea*
[4]*School of Electrical and Electronics Engineering, Chung-Ang University, Seoul 06910, Republic of Korea*

Correspondence should be addressed to Jong-Suk Ro; jongsukro@gmail.com

Received 23 February 2022; Revised 29 March 2022; Accepted 8 April 2022; Published 5 May 2022

Academic Editor: Reza Hamidi



Power System of the age has included remarkable contribution of distributed energy resources (DERs). This inclusion has opened new era of research and studies. Islanding detection has become one of the important events in power system that is to be detected precisely. This study introduces a single-parameter-based passive technique for islanding detection which has zero nondetection zone without involvement of any signal processing tool. The proposed technique is tested for various islanding and nonislanding events. The simulation results prove that the suggested technique detects islanding event accurately and it is capable of distinguishing islanding and nonislanding events by an economical and simpler method.

## 1. Introduction

Depleting conventional energy resources and increased demand of energy has led researchers towards the use of distributed energy resources (DERs) [1]. Therefore, DERs addition in power system is increasing day by day. But this integration has created new complications in the power system. Islanding is one of the power system disturbance that is defined as follows: "It is the situation when grid trips out but DERs remain connected with the system." This affects power quality of the system and endangers the life of utility staff working for the restoration of the system supply [2]. Therefore, it is one of the issues which is to be tackled promptly. According to IEEE Std. 1547, Distributed Generation Source should detect islanding condition and become disconnected from the system within 2 sec [3].

*1.1. Literature Review.* Generally, islanding detection techniques are classified into two parts, remote and local [4]. Remote techniques work on the basis of communication signal between DGs and the utility network [4, 5]. These are considerably more reliable techniques but expensive due to involvement of communication devices. For example, Switch State Monitoring [6] and Intertripping [7, 8] are the remote techniques which are more reliable and avoid nondetection zone but due to the involvement of communication system (SCADA), they are very expensive.

Local techniques involve the measurement of system parameters like voltage, frequency, current, and harmonic distortion at the site of DGs. No communication equipment is required for any interaction between breakers and generating units. Therefore, local techniques are considered less expensive and more economical for islanding detection in distribution system containing DGs. The local techniques are further divided into active, passive, and hybrid techniques [5, 9, 10].

Active techniques [4, 5, 11] involve such methods of islanding detection in which small disturbances are introduced to the system. Disturbance signal is sent and received

periodically between PV inverter and grid which continuously monitors whether the inverter and grid are tied or not. Impedance measurement [12], Slip Mode Frequency Shift (SMS) [13], Active Frequency Drift (AFD) [14], Sandia Frequency Drift (SFS) [15, 16], and Sandia Voltage Shift (SVS) [17] are some examples of active techniques. These are comparatively more effective than passive techniques because of smaller nondetection zone but have main limitation on disturbance added to the system. Therefore active methods have three drawbacks. Firstly, the added disturbance affects power quality of the system, secondly extra time is needed to collect the response of the system for the added disturbance, and thirdly complexity of the system is increased.

In passive techniques, some parameters at point of common coupling are monitored [18] and the sample values are compared with predefined threshold values. Such methods do not disturb power quality but exhibit large nondetection zone as compared to active techniques. These techniques are preferred due to low implementation cost, simplicity, and no negative impact on grid operation [19, 20].

The most popular passive techniques being used involve following parameters in different combinations, under/overvoltage, under/overfrequency, rate of change of voltage, rate of change of frequency, rate of change of reactive power [21], phase jump detection, rate of change of frequency with power, rate of change of power with total harmonic distortion, voltage unbalance and total harmonic distortion of current signal, voltage and power factor change, frequency shift in combination with voltage and total harmonic distortion of voltage, etc. To decrease larger nondetection zone of passive methods, advanced signal processing tools such as Duffing oscillations, wavelet transforms, and S-transform are employed. Machine learning techniques are also being used in islanding detection like support vector machine (SVM) based methods [2, 22]. The information produced after signal processing is used to identify islanding condition with the help of classifiers. Intelligent classifiers used are artificial neural network (ANN), probabilistic neural network (PNN), decision tree, and fuzzy logic [23]. The hybrid methods combine the advantages of active and passive methods and leave out their shortages [24].

*1.2. Research Gaps.* Here is a common feature of all earlier presented islanding detection techniques that the power system model adopted is comprised of concentrated form of load. But ground reality of the field study shows that load of a feeder is distributed along the length of the feeder. The concentrated-load consideration obviously decreased the complexity of the system model but it has increased the complication of islanding detection techniques and deviated away the attention from ground realities.

Distribution system of different utility companies has been studied for better estimation of the system in modeling consideration. It is unanimously found in all distribution companies that the load of the area exists in distributed manner rather than concentrated form. Second important information exposed that the load attached or demand of the area where DG exists is quiet higher than the generation capacity of the DG. In other words it can be explained as the power delivered by grid at any time during normal operating conditions is many times higher than the generation of the DGs. So power flow direction at any time during normal operation will be from grid to the point of common coupling (PCC).

*1.3. How This Paper Fills the Gaps.* In author's opinion, the performance of feeder with concentrated load does not represent the ground realities. So, model of distribution system is prepared as per ground reality of the field. It contains 11 kV feeder with utility grid source and distributed energy sources (DERs). The DERs consist of solar PV plant and mini hydro plants. The load of the feeder is modeled in distributed form for better estimation of the real feeder. Three different loads have been placed at different locations of the feeder. The performance of the feeder with distributed load is analyzed for islanding and nonislanding events.

*1.4. Contribution of This Paper.* Main contribution of this paper is that it proposes single parameter "reverse power" based islanding detection technique which is newly being introduced as per author's knowledge. This is very simple, inexpensive, and accurate passive technique. This has no involvement of signal processing, classifiers, or machine learning algorithm and can be easily implemented in any power system. Another unique feature of this paper is that despite being passive technique and noninvolvement of signal processing methods, it has zero nondetection zone. Many loading conditions and nonislanding events have been tested but this technique is not malfunctioned anyway. Therefore, it is very simple, cheap, intelligent, and accurate technique having zero nondetection zone.

## 2. Materials and Method

A simple 11 kV system as shown in Figure 1 is modeled in PSCAD consisting of DGs on one side and the grid on the other side. DGs consist of two solar PV plants (0.5 MW each) and two mini hydro plants (2 MW each). The mini hydro plants are comprised of synchronous generators. Load is distributed in three parts between DGs and grid.

So, according to real field study the load is modeled in distributed form and the demand of the area is considered higher than the generation of the DGs existing in that area. A 6 MW load is connected between solar PV plants and mini hydro plants; two loads of 6 MW and 9 MW are connected between DGs and the grid. The detail of system parameters is given in Table 1.

The 11 kV system model is simulated in PSCAD and power flow is monitored at every branch and especially at PCC of DGs. During islanding and nonislanding cases, many of the parameters like real power, reactive power, voltage, current, and frequency of the system have been monitored at PCC during the simulation. Islanding situation

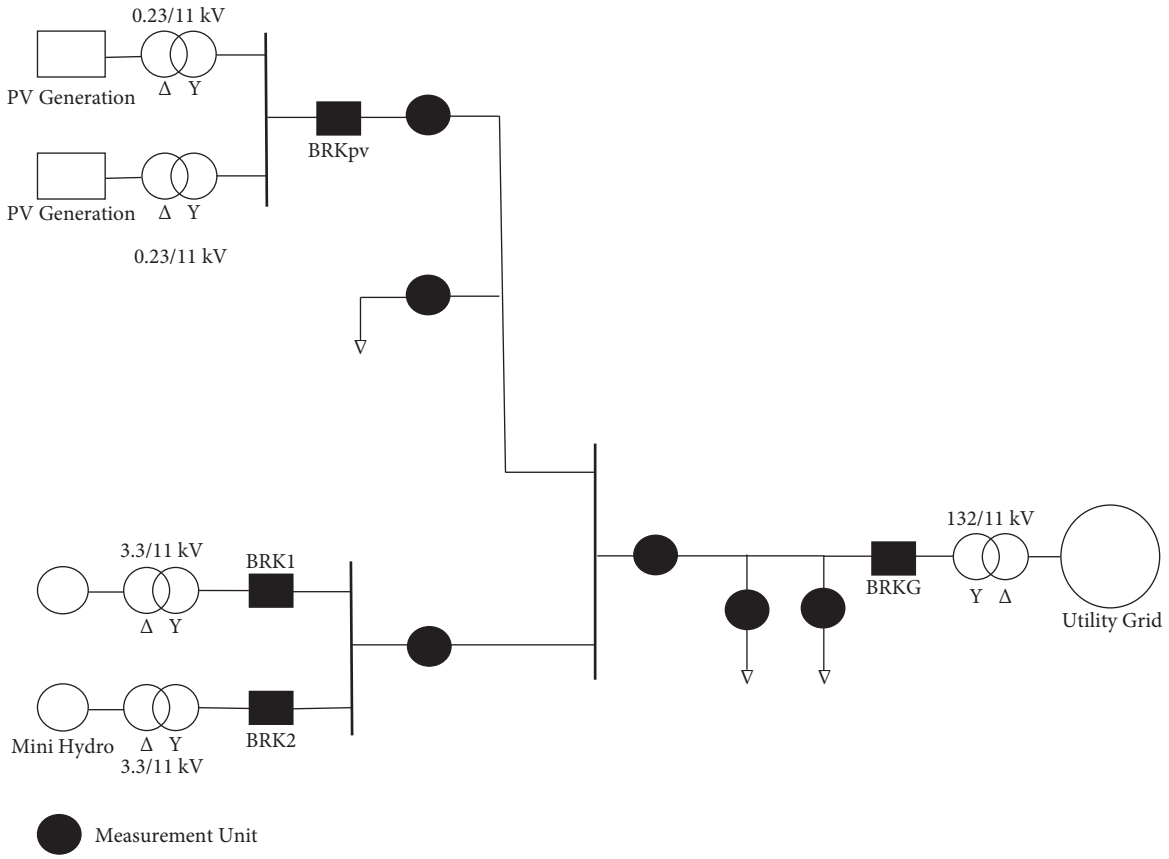


Figure 1: Single line diagram of the 11 kV power system model.

Table 1: System parameters used in model.

| | |
|---|---|
| Grid | $V = 132$ kV, $f = 50$ Hz |
| Common feeder | $V = 11$ kV, $f = 50$ Hz |
| PV generation | $P = 2 \times 0.5$ MW, $V = 230$ V |
| Mini hydro | $P = 2 \times 2$ MW, $V = 3.3$ kV, $f = 50$ Hz |
| Grid transformer | $S = 20$ MVA, $V = 132/11$ kV, $f = 50$ Hz |
| PV generation transformer | $S = 1$ MVA, $V = 0.23/11$ kV, $f = 50$ Hz |
| Mini hydro transformer | $S = 2 \times 2$ MVA, 3.3/11 kV, $f = 50$ Hz |
| DG side load | $P = 6$ MW, $Q = 3$ MVAR, $V = 11$ kV |
| Grid side load | $P = 15$ MW, $Q = 4$ MVAR, $V = 11$ kV |
| Induction motor | $P = 1$ MW, $V = 11$ kV |
| Capacitor bank | $Q = 1$ MVAR, $V = 11$ kV |
| Short circuit fault | $R = 0.01$ ohm |

is created by tripping grid side breaker (BRKG) and change in parameters is observed for different loading conditions.

## 3. Feature Selection

Single line diagram of the 11 kV system model in Figure 1 contains 5 MW DGs' generation. The demand of the area where DGs are located is 6 MW. About 1 MW power will be delivered by the grid towards PCC. This model fulfills both of our considerations shown in real field study that the load is in distributed form and secondly the demand of the area is higher than generation capacity of DGs. In other words, grid support is essential to meet the area demand. During normal operation, the direction of power flow will be towards PCC which is taken as positive real power. When islanding occurs, the grid will stop feeding the load. But grid side load is still connected with the system and DGs are also connected with the system. So the power flow direction at PCC will change instantaneously. It will be now from PCC to grid side load which will be taken as negative or reverse power. Analysis of this real world based power system model facilitates in the manner that only reverse power monitored at PCC is adequate for islanding detection. The reversal of power flow will be able to identify the islanding event clearly.

## 4. Algorithm

As the focus was to select only single parameter which must surely detect islanding condition, on the basis of model analysis, real power P is selected to test for different islanding and nonislanding conditions.

The algorithm used during testing is presented in process flow diagram shown in Figure 2 which specifies the power flow measurement procedure and decision taking strategy of the technique. Power ($P$) is measured during the process and the threshold value of the power ($P_{\text{th}}$) is compared to take decision. A time delay of 0.2 sec is kept to ensure that the reversal in power flow direction has certainly occurred only due to islanding event and not due to any nonislanding event like Earth fault condition between PCC and the grid.

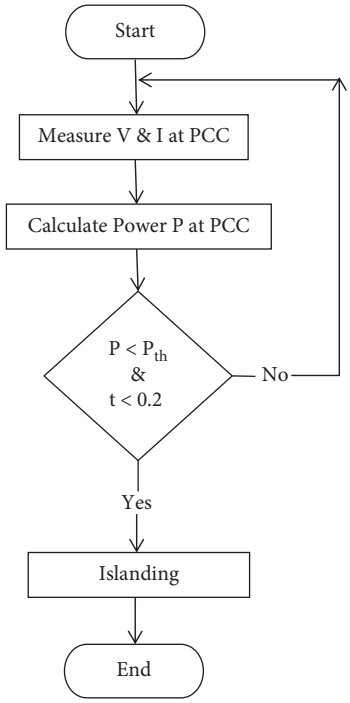


Figure 2: Process flowchart of reverse power islanding detection technique.

The single parameter, "reverse power," has been tested for different islanding and nonislanding cases simulated in PSCAD. The outcomes of simulations as per algorithm given in Figure 2 have been recorded. Casewise observations are hereby discussed in detail.

## 5. Case Studies

*5.1. Islanding Detection with Reverse Power.* Model shown in Figure 1 is designed and simulated in PSCAD environment. Islanding condition is created by tripping Grid Side Circuit Breaker (BRKG). Before islanding, under normal working conditions, power flow at PCC is from grid to PCC which is taken as positive. As islanding occurs (i.e., Grid Circuit Breaker (BRKG) trips) the power flow direction suddenly changes and becomes negative, meaning that the power flow direction is reversed and now it is from PCC towards grid side load.

The graph in Figure 3 is showing simulation result of power flow direction at PCC with respect to time. The simulation is started at time 0 sec; the system is trying to stabilize itself from 0 to 1.3 sec. From 1.3 sec to 3 sec, the system is working under normal conditions and the 1.17 MW power flow is from grid to PCC. At time 3 sec, grid breaker (BRKG) trips and graph show that power flow direction is suddenly changed from 1.17 MW to −4.89 MW. From time 3 sec to onward the graph is showing reverse power. The continuous variation in reverse power indicates that the system is now unstable. In this case, the graph clearly shows that reverse power appeared instantly at PCC as islanding has occurred. So this illustrates that single parameter (reverse power $P$ at PCC) has detected islanding event promptly and precisely.

*5.2. Nonislanding Events.* Nonislanding events are created between PCC and DGs side as well as between PCC and grid side. When these events occur between PCC and DGs, power flow from grid to PCC, i.e., positive power, is increased. So, nonislanding events cannot create reversal of power at PCC anyway. Therefore, the reverse power parameter at PCC is tested for various nonislanding cases occurring between PCC and grid. The summary of results is shown in Table 2.

As capacitor switching is the normal routine event which occurs in any small or big industry, at the start of each working day, capacitors are switched on and with the end of working day they are switched off. Hence capacitors switching (on/off) events are necessary to be tested for reverse power response. So 1 MVAR capacitor switching events have been created at the feeder part between PCC and grid during simulation of Figure 1 model in PSCAD. The simulation result for the reverse power at PCC is shown in graph of Figure 4. Capacitor is switched on at time 3 sec and switched off at time 5 sec during simulation. The graph of Figure 4 shows a little variation at switching events only. But reverse power does not appear at PCC during 1 MVAR capacitor switching. It proves that capacitor switching does not create reverse power at PCC.

The literature of induction motor shows that its starting current in some cases becomes higher than its full load current. Therefore, induction motor starting event seems compulsory to be tested for reverse power observation at PCC. In this regard, startup event of 1.2 MW induction motor is created at the feeder part between PCC and grid during simulation of Figure 1 model in PSCAD. The simulation result for the reverse power at PCC is represented in graph of Figure 5. Induction motor is started at time 3 sec; the graph shows that a little variation has occurred in the positive power at PCC at time 3 sec but reverse power has not during startup of 1.2 MW induction motor. So, this nonislanding event has also proved that reverse power has not occurred at PCC due to startup event of induction motor.

Other possible nonislanding events which may occur in case of power system faults (as from Sr.4 to 8 of Table 2) have also been simulated to observe reverse power flow at PCC. In LG, LL, and LLL fault cases, reverse power is not observed at point of common coupling (PCC) even for 0.01 sec as shown in Figures 6–8. During LL-G fault, instantaneous reverse power up to 0.15 MW is seen for 0.01 sec as shown in Figure 9 and during LLLG fault the reverse power of 0.29 MW observed for 0.033 sec as shown in Figure 10.

*5.3. Weak Grid Conditions and Islanding Detection by Reverse Power.* The power system is inspected by many of its parameters like voltage level, frequency, active power, reactive power, and apparent power. The stability of the power system is observed by stability of voltage and frequency. If voltage and frequency of the system are stable under specific loading conditions, the power system is considered as a stable power system. If variations are observed in voltage or frequency of the system then such system is not considered a stable power system. When the power system is integrated

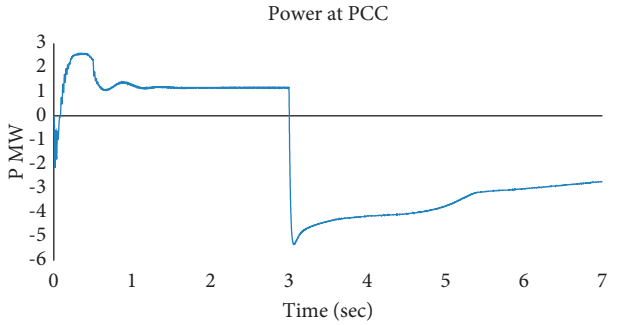


Figure 3: Power flow direction being monitored before and after islanding event.

Table 2: Nonislanding cases.

| Sr. No | Case description | Reverse power |
|---|---|---|
| 1 | Capacitor (1 MVAR) switching | No |
| 2 | Induction motor (1.2 MW) starting | No |
| 3 | Load switching | No |
| 4 | Single phase to ground fault (L-G) | No |
| 5 | Phase to phase fault (LL) | No |
| 6 | Phase to phase and ground fault (LL-G) | Yes |
| 7 | Three-phase fault (LLL) | No |
| 8 | Three-phase to ground fault (LLL-G) | Yes |

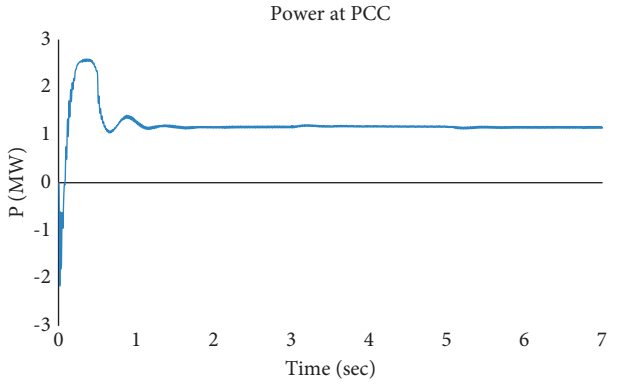


Figure 4: Capacitor (1.0 MVAR) switched on at $t = 3$ sec and switched off at $t = 5$ sec.

with distributed generators (DGs) having variations in voltage and frequency then this situation is taken as weak grid. The weakness of grid can be defined in terms of short circuit ratio (SCR) [25].

$$\text{SCR} = \frac{S_{CC}}{S_N}, \tag{1}$$

where SCR = short circuit ratio, $S_{CC}$ = short circuit power capability of the system at point of common coupling (PCC), $S_N$ = rated power of distributed generator installed.

The weak grid condition is mathematically measured by short circuit ratio (SCR) which is the ratio of short circuit power capability at the point of common coupling and the rated power of distributed generators installed at the point. If SCR is less than 10, the grid is considered weak. When SCR is

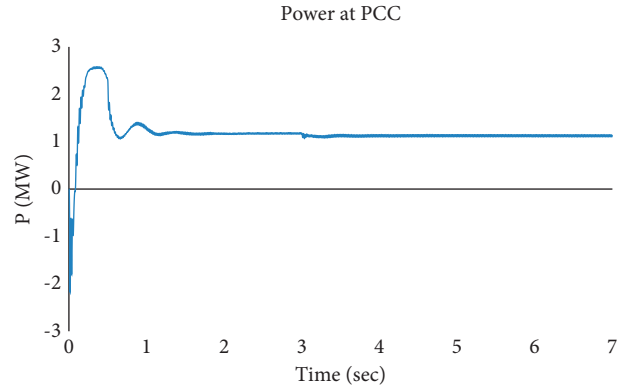


Figure 5: Induction motor with 1.2 MW load is switched on at $t = 3$ sec.

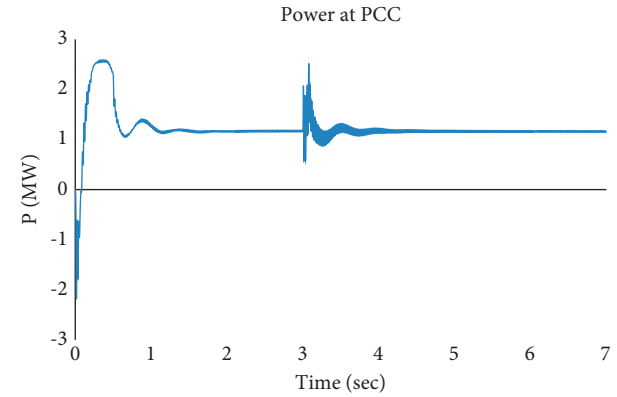


Figure 6: LG fault occurred at $t = 3$ sec for duration of 0.05 sec.

greater than 20, the grid is considered strong. The short circuit power capability SCC at point of common coupling is given by

$$S_{CC} = \frac{U_g^2}{Z_g}, \tag{2}$$

where $U_g$ is rated voltage of grid and $Z_g$ is impedance of grid.

By equations (1) and (2)

$$\text{SCR} = \frac{U_g^2}{Z_g \cdot S_N}. \tag{3}$$

Weak grid conditions are produced here to identify whether the reverse power parameter is sufficient for islanding detection or not. Secondly, threshold value of reverse power is to be identified for the model under study. The above explanation justifies that weak grid condition can be achieved by minimizing the grid power which will decrease the numerator of equation (1). Decrease in numerator value will decrease the short circuit ratio (SCR).

So, here we have achieved the weak grid condition by minimizing the grid input power gradually. The grid side load is also minimized to keep supply-demand balance in the

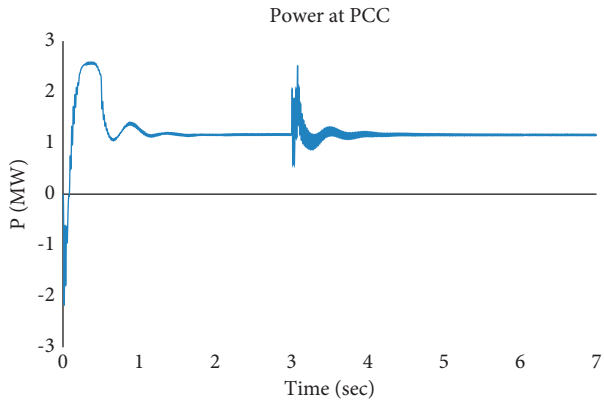


Figure 7: LL fault occurred at $t = 3$ sec for duration of 0.05 sec.

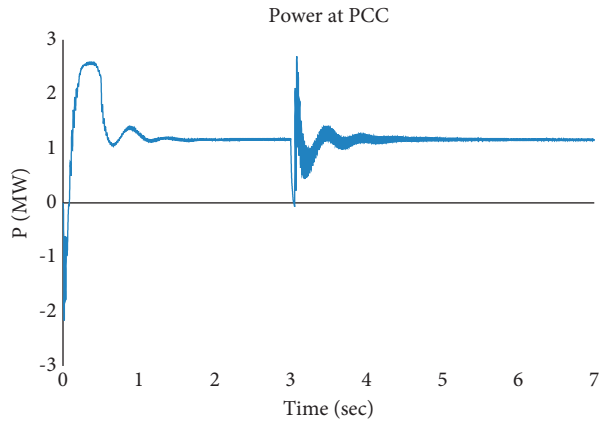


Figure 8: LLL fault occurred at $t = 3$ sec for duration of 0.05 sec.

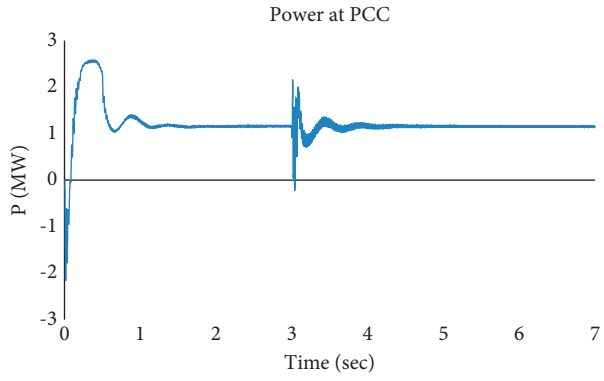


Figure 9: LLG fault occurred at $t = 3$ sec for duration of 0.05 sec.

system. For this purpose 10 events have been created during which grid input power is minimized gradually from 15.58 MW to 1.56 MW while DGs input is kept constant at 4.7 MW. DG side generation and load have not been varied considering that the DGs side load is the least demand of the area. Without islanding event, reverse power is not observed during any of the weak grid situations. However it is observed that when islanding event occurs under weak grid conditions the value of reverse power is getting decreased, respectively, as the grid input is being reduced. The

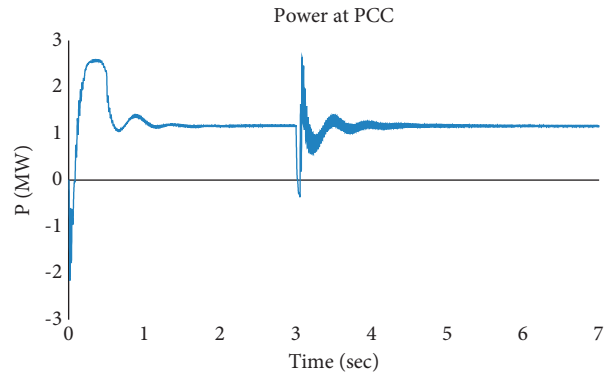


Figure 10: LLLG fault occurred at $t = 3$ sec for duration of 0.05 sec.

reduction in reverse power is due to the fact that the minimum grid support feeds small part of load and DGs has to overcome this small part during islanding event. The list of weak grid events and results is shown in Table 3.

*5.4. Nondetection Zone of Reverse Power Based Islanding Detection Technique.* The reverse power based islanding detection technique uses direction of active power flow from DGs to the grid side load at point of common coupling (PCC). It does not involve any influence of frequency variation or voltage fluctuation in islanding detection process as shown in process flow diagram in Figure 2. This technique has no NDZ according to equations (4) and (5) [26, 27]. So despite being a passive technique, this has zero NDZ.

$$Q_f \cdot \left(1 - \left(\frac{f}{f_{\min}}\right)^2\right) \leq \frac{\Delta Q}{P} \leq Q_f \cdot \left(1 - \left(\frac{f}{f_{\max}}\right)^2\right), \quad (4)$$

$$\left(\frac{V}{V_{\max}}\right)^2 - 1 \leq \frac{\Delta P}{P} \leq \left(\frac{V}{V_{\min}}\right)^2 - 1. \quad (5)$$

*5.5. Comparison of Reverse Power Islanding Detection with Other Parameters.* Many of the passive islanding detection techniques have been presented up till now. Most of them involve the performance of voltage, frequency, ROCOV, and ROCOF like parameters alone or in different combinations with other parameters like active and reactive power at PCC for islanding detection. In this paper, we have presented a novel technique based on single parameter "reverse power" that is being monitored at PCC.

For comparison of performance of earlier used parameters with reverse power parameter, we have simulated an islanding event for the model of Figure 1 during which the power mismatch is kept very small. In this case, DGs generation is 4.683 MW and total load of the system is 4.8552 MW; i.e., grid input is 0.18 MW which is very small as compared to the load demand. The system parameters are given in detail in Table 4.

The simulation starts at time 0 sec and system tries to stabilize itself up to time 2.7 sec due to which variations are observed initially in graphs of all figures. When islanding

Table 3: Weak grid conditions and islanding detection by reverse power.

| Sr. No | DGs input power | | Grid input power | | Load | | Total generation | | Reverse power upon islanding |
|---|---|---|---|---|---|---|---|---|---|
| | *P* (MW) | *Q* (MVAR) | P (MW) | *Q* (MVAR) | *P* (MW) | *Q* (MVAR) | *P* (MW) | *Q* (MVAR) | *P* (MW) |
| 1 | 4.7226 | 4.111 | 15.58 | 3.806 | 20.267 | 6.686 | 20.3026 | 7.917 | −5.25 |
| 2 | 4.7346 | 4.3736 | 14.39 | 5.251 | 18.857 | 8.343 | 19.1246 | 9.6246 | −4.8 |
| 3 | 4.6954 | 3.9044 | 11.43 | 3.84 | 16.099 | 6.5642 | 16.1254 | 7.7444 | −4.64 |
| 4 | 4.7266 | 3.5758 | 10.02 | 3.25 | 14.71 | 5.734 | 14.7466 | 6.8258 | −4.54 |
| 5 | 4.7484 | 3.4796 | 7.1 | 3.41 | 11.802 | 5.745 | 11.8484 | 6.8896 | −3.5 |
| 6 | 4.7472 | 3.1606 | 4.212 | 2.326 | 8.923 | 4.38 | 8.9592 | 5.4866 | −2.21 |
| 7 | 4.701 | 3.0354 | 3.648 | 2.143 | 8.305 | 4.117 | 8.349 | 5.1784 | −1.86 |
| 8 | 4.7372 | 3.001 | 3.038 | 2.163 | 7.714 | 4.094 | 7.7752 | 5.164 | −1.4 |
| 9 | 4.7202 | 2.9824 | 2.465 | 1.921 | 7.154 | 3.8363 | 7.1852 | 4.9034 | −0.98 |
| 10 | 4.7186 | 7.3926 | 1.595 | 1.431 | 3.2701 | 3.1789 | 6.3136 | 8.8236 | −0.26 |

Table 4: System parameters during islanding event with small power mismatch.

| DGs input power | | Grid input power | | Load | | Total generation | | Reverse power upon islanding |
|---|---|---|---|---|---|---|---|---|
| *P* (MW) | *Q* (MVAR) | *P* (MW) | *Q* (MVAR) | *P* (MW) | *Q* (MVAR) | *P* (MW) | *Q* (MVAR) | *P* (MW) |
| 4.683 | 2.39 | 0.1897 | 0.853 | 4.8552 | 2.939 | 4.8727 | 3.243 | −0.143 |

occurred at time 5 sec, the reverse power is noted −0.143 MW permanently as shown in Figure 11; this detects the islanding event correctly.

During islanding, change in system voltage is observed at PCC, which is from 1 pu to 0.98 pu as shown in Figure 12. This depicts that the voltage variation is under tolerable limits and cannot identify the islanding event.

The frequency of the system at PCC during islanding event is observed which varies from 50 Hz to 49.67 Hz as shown in Figure 13. So the frequency variation is also under tolerance limits and it is unable to find the islanding event.

The rate of change of voltage (ROCOV) and rate of change of frequency (ROCOF) are also inspected which are very small at time 5 sec as shown in Figures 14 and 15 and they are incapable of identifying the islanding condition.

So the islanding event during small power mismatch shows that change in voltage, change in frequency, ROCOV, and ROCOF have failed to identify the islanding event but reverse power at PCC has clearly identified the event. Therefore, reverse power parameter is proved more effective for the identification of islanding condition.

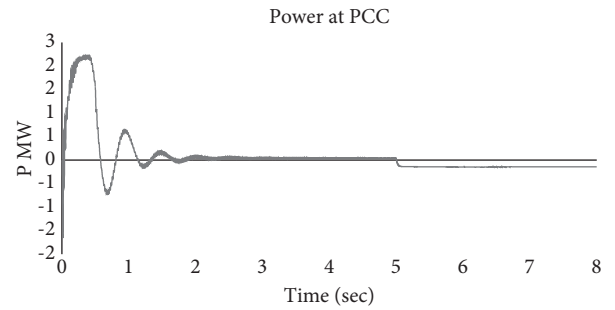


Figure 11: Power at PCC during islanding event with small power mismatch.

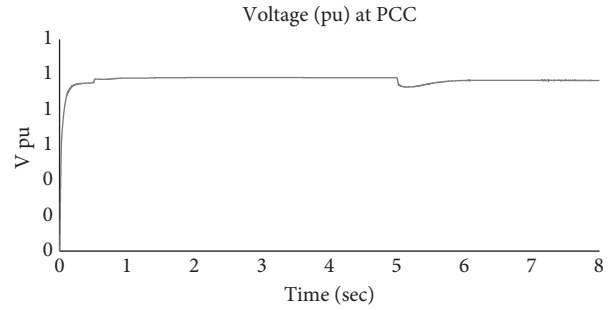


Figure 12: Voltage at PCC during islanding event with small power mismatch.

## 6. Results

The simulation results of the model in Figure 1 shown in Table 2 indicate that reverse power parameter remains inactive during any of the nonislanding events except LL-G and LLL-G faults. The results shown in Table 3 verify that reverse power parameter does not malfunction during weak grid condition against the algorithm given in Figure 2. The reverse power only appears when islanding occurs actually. Under LL-G fault condition as represented in Figure 9, reverse power up to 0.15 MW is observed for 0.01 sec at PCC and during LLL-G fault as in Figure 10, 0.29 MW reverse power is observed for 0.033 sec at PCC. Reverse power in LL-G and LLL-G faults is for very short time while under islanding condition, reverse power occurs permanently as simulation result indicates in Figure 3. Therefore, time delay of 0.2 sec is incorporated in reverse power to avoid the confusion that might be produced by LL-G or LLL-G faults. Results are evident that the delay of 0.2 sec is sufficient to clearly discriminate islanding event from nonislanding.

The simulation results depicted in Table 4 and Figures 11 to 15 for the comparison of parameters' performance during islanding event under small power mismatch condition are also evidence that frequency and voltage based techniques

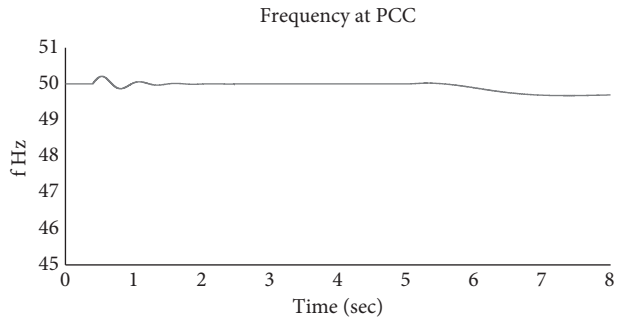


Figure 13: Frequency at PCC during islanding event with small power mismatch.

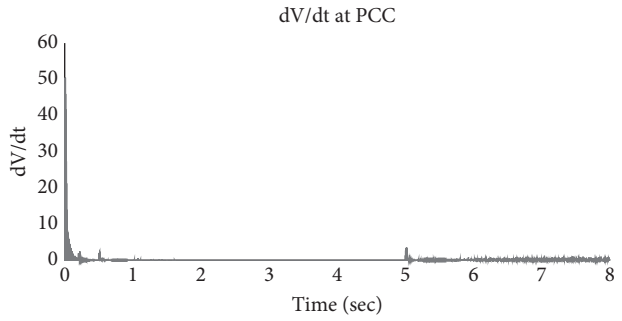


Figure 14: ROCOV at PCC during islanding event with small power mismatch.

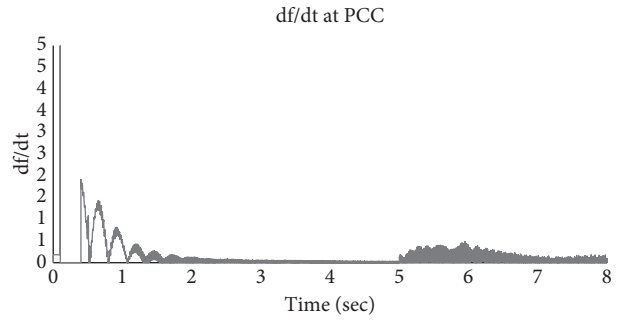


Figure 15: ROCOF at PCC during islanding event with small power mismatch.

have failed to work but reverse power has worked very accurately under the same conditions.

So it is clear from all results that reverse power is sufficient to detect islanding event and discriminates any of the islanding events from nonIslanding events in intelligent way. During weak grid situation and small power mismatch case, the grid input power is lessened and less load is being fed from grid so power mismatch is very small. Therefore, the value of reverse power is decreased due to little power mismatch. But still reverse power parameter at PCC is surely capable of detecting islanding event clearly. The threshold value of reverse power is zero for islanding detection under all conditions. In this way, the single parameter "reverse power" with time delay of 0.2 sec is capable of detecting the islanding event and discriminating islanding event from all nonislanding events.

## 7. Discussion

Reverse power parameter is already being used in protection scheme of conventional power plants connected with national grid. Our proposed method proves that it is also helpful in DGs' case and is capable of isolating DGs from islanded system. As none of the signal processing tools is involved in this technique, it has minimized delay in operation and more accurately detects the islanding event. Results show that our proposed technique detects islanding event in 0.2 sec by single parameter "reverse power at PCC." Therefore, it follows IEEE Std. 1547 that distributed generator should detect islanding condition and isolate the DGs within 2 sec. No classifier is involved in this technique, so there is no need of training data and no additional time is required for making decision.

Although it is passive technique its nondetection zone (NDZ) is zero because voltage and frequency are not involved in islanding detection process. During case studies, any of the nonislanding events did not tend to impair the detection results. So the quick detection, zero NDZ, and simple implementation make it a unique islanding detection technique which is cheaper, simpler, single-parameter-based, and intelligent as compared to all other passive and active islanding detection techniques.

## Nomenclature

| | |
|---|---|
| DER: | Distributed energy resources |
| IEEE: | Institute of Electrical and Electronics Engineers |
| SCADA: | Supervisory control and data acquisition |
| DG: | Distributed generator |
| SMS: | Slip Mode Frequency Shift |
| AFD: | Active frequency drift |
| SFS: | Sandia frequency drift |
| SVS: | Sandia voltage shift |
| PCC: | Point of common coupling |
| WAPDA: | Water and power development authority |
| NTDC: | National Transmission and Dispatch Company |
| NPCC: | National Power Control Center |
| DISCO: | Distribution companies |
| GENCO: | Generation companies |
| NDZ: | Nondetection zone |
| WT: | Wave transform |
| DWT: | Discrete wave transform |
| FT: | Fourier transforms |
| FFT: | Fast Fourier transform |
| ANN: | Artificial neural network |
| PNN: | Probabilistic neural network |
| DT: | Decision tree |
| ROCOV: | Rate of change of voltage |
| ROCOF: | Rate of change of frequency |
| SCR: | Short circuit ratio |
| $S_{CC}$: | Short circuit power capability of the system at point of common coupling (PCC) |
| $S_N$: | Rated power of distributed generator installed |
| $U_g$: | Rated voltage of grid |
| $Z_g$: | Impedance of grid |
| P: | Active power |

$\Delta P$, $\Delta Q$: Active, reactive power mismatch.

## Data Availability

No data were used to support this study.

## Conflicts of Interest

The authors declare that they have no conflicts of interest.

## Acknowledgments

This research was supported by the Basic Science Research Program through the National Research Foundation of Korea funded by the Ministry of Education (2016R1D1A1B01008058), National Research Foundation of Korea (NRF) Grant funded by the Korea government (MSIT) (no. NRF-2022R1A2C2004874), and the Brain Pool Program through the NRF of Korea funded by the Ministry of Science and ICT (2019H1D3A1A01102988).

## References

[1] S. Sivanandan, V. R. Pandi, and K. Ilango, "Energy management of a smart building integrated with distributed energy resources," in *Proceedings of the 2017 Innovations in Power and Advanced Computing Technologies (i-PACT)*, Vellore, India, April 2017.

[2] H. R. Baghaee, D. Mlakic, S. Nikolovski, and T. Dragicevic, "Anti-islanding protection of PV-based microgrids consisting of PHEVs using SVMs," *IEEE Transactions on Smart Grid*, vol. 11, no. 1, pp. 483–500, 2020.

[3] J. C. Boemer, M. Huque, B. Seal, T. Key, D. Brooks, and C. Vartanian, "Status of revision of IEEE Std 1547 and 1547.1," in *Proceedings of the 2017 IEEE Power & Energy Society General Meeting*, Chicago, IL, USA, July 2017.

[4] A. G. Abokhalil, A. Awan, and A. Al-Qawasmi, "Comparative study of passive and active islanding detection methods for PV grid-connected systems," *Sustainability*, vol. 10, no. 6, p. 1798, 2018.

[5] T.-Z. Bei, "Accurate active islanding detection method for grid-tied inverters in distributed generation," *IET Renewable Power Generation*, vol. 11, no. 13, pp. 1633–1639, 2017.

[6] A. Khamis, H. Shareef, E. Bizkevelci, and T. Khatib, "A review of islanding detection techniques for renewable distributed generation systems," *Renewable and Sustainable Energy Reviews*, vol. 28, pp. 483–493, 2013.

[7] D. Kumar, "A survey on recent developments of islanding detection techniques," *Turkish Journal of Electrical Power and Energy Systems*, vol. 1, pp. 42–53, 2021.

[8] B. Hariprasad, P. Bharat Kumar, P. Sujatha, and G. Sreenivasan, "A novel adaptive rule-based islanding detection technique for voltage source inverter-based distribution generation," *Journal of Green Engineering*, vol. 11, pp. 511–529, 2021.

[9] C. H. Rami Reddy and K. Harinadha Reddy, "An efficient passive islanding detection method for integrated DG system with zero NDZ," *International Journal of Renewable Energy Resources*, vol. 8, no. 4, pp. 1994–2002, 2018.

[10] R. Zamani, M. E. Hamedani Golshan, H. Haes Alhelou, and N. Hatziargyriou, "A novel hybrid islanding detection method using dynamic characteristics of synchronous generator and signal processing technique," *Electric Power Systems Research*, vol. 175, Article ID 105911, 2019.

[11] B. Indu Rani, M. Srikanth, G. Saravana Ilango, and C. Nagamani, "An active islanding detection technique for current controlled inverter," *Renewable Energy*, vol. 51, pp. 189–196, 2013.

[12] M. Roop, J. Ginn, J. Stevens, W. Bower, and S. Gonzales, "Simulation and experimental study of the impedance detection anti-islanding method in the single inverter case," in *Proceedings of the Fourth World Conference on Photovoltaic Energy Conference*, pp. 2379–2382, Waikoloa, HI, USA, May 2006.

[13] M. Bahador, M. Zareie, S. Eren, and M. Pahlevani, "Stability analysis of the slip mode frequency shift islanding detection in single phase PV inverters," in *Proceedings of the 2017 IEEE 26th International Symposium on Industrial Electronics (ISIE)*, Edinburgh, UK, June 2017.

[14] S. Shrivastava, S. Jain, R. K. Nema, and V. Chaurasia, "Two level islanding detection method for distributed generators in distribution networks," *International Journal of Electrical Power & Energy Systems*, vol. 87, pp. 222–231, 2017.

[15] R. Azim, F. Li, Y. Xue, M. Starke, and H. Wang, "An islanding detection methodology combining decision trees and Sandia frequency shift for inverter-based distributed generations," *IET Generation, Transmission & Distribution*, vol. 11, no. 16, pp. 4104–4113, 2017.

[16] A. Y. Hatata, E.-H. Abd-Raboh, and B. E. Sedhom, "Proposed Sandia frequency shift for anti-islanding detection method based on artificial immune system," *Alexandria Engineering Journal*, vol. 57, no. 1, pp. 235–245, 2018.

[17] M. El-Moubarak, M. Hassan, and A. Faza, "Performance of three islanding detection methods for grid-tied multi-inverters," in *Proceedings of the 2015 IEEE 15th International Conference on Environment and Electrical Engineering (EEEIC)*, Rome, Italy, June 2015.

[18] Ch R. Reddy, B. Srikanth Goud, B. Nagi Reddy, M. Pratyusha, C. V. Vijay Kumar, and R. Rekha, "Review of islanding detection parameters in smart grids," in *Proceedings of the 2020 8th International Conference on Smart Grid*, Paris, France, June 2020.

[19] P. Mahat, Z. Chen, and B. Bak-jensen, "Review on islanding operation of distribution system with distributed generation," in *Proceedings of the Power and Energy Society General Meeting*, pp. 1–8, Detroit, MI, USA, July 2011.

[20] B. K. Panigrahi, A. Bhuyan, J. Shukla, P. K. Ray, and S. Pati, "A comprehensive review on intelligent islanding detection techniques for renewable energy integrated power system," *International Journal of Energy Research*, vol. 45, no. 10, pp. 14085–14116, 2021.

[21] S. Nikolovski, H. R. Baghaee, and D. Mlakić, "Islanding detection of synchronous generator-based DGs using rate of change of reactive power," *IEEE Systems Journal*, vol. 13, no. 4, pp. 4344–4354, 2019.

[22] H. R. Baghaee, D. Mlakic, S. Nikolovski, and T. Dragicevic, "Support vector machine-based islanding and grid fault detection in active distribution networks," *IEEE Journal of Emerging and Selected Topics in Power Electronics*, vol. 8, no. 3, pp. 2385–2403, 2020.

[23] D. Mlakić, H. R. Baghaee, and S. Nikolovski, "A novel ANFIS-based islanding detection for inverter-interfaced microgrids," *IEEE Transactions on Smart Grid*, vol. 10, no. 4, pp. 4411–4424, 2019.

[24] D. Mlakić, H. R. Baghaee, and S. Nikolovski, "Gibbs phenomenon-based hybrid islanding detection strategy for VSC-

based microgrids using frequency shift, $ THD_ {U} $, and $ RMS_ {U}$," *IEEE Transactions on Smart Grid*, vol. 10, no. 5, pp. 5479–5491, 2018.

[25] S. L. Lorenzen, A. B. Nielsen, and L. Bede, "Control of a grid connected converter during weak grid conditions," in *Proceedings of the 2016 IEEE 7th International Symposium on Power Electronics for Distributed Generation Systems (PEDG)*, Vancouver, BC, Canada, June 2016.

[26] M. Y. Worku, M. A. Hassan, L. S. Maraaba, and M. A. Abido, "Islanding detection methods for microgrids: a comprehensive review," *Mathematics*, vol. 9, no. 24, p. 3174, 2021.

[27] Z. Ye, A. Kolwalkar, Y. Zhang, P. Du, and R. Walling, "Evaluation of anti-islanding schemes based on non-detection zone concept," *IEEE Transactions on Power Electronics*, vol. 19, no. 5, pp. 1171–1176, 2004.